



# Metabolomic profiling of human bladder tissue extracts

Krzysztof Ossoliński<sup>1</sup> · Tomasz Ruman<sup>2</sup> · Valérie Copié<sup>3</sup> · Brian P. Tripet<sup>3</sup> · Artur Kołodziej<sup>2</sup> · Aneta Płaza-Altamer<sup>2</sup> · Anna Ossolińska<sup>1</sup> · Tadeusz Ossoliński<sup>1</sup> · Zuzanna Krupa<sup>4</sup> · Joanna Nizioł<sup>2</sup>

Received: 26 May 2023 / Accepted: 1 December 2023 / Published online: 24 January 2024  
© The Author(s), under exclusive licence to Springer Science+Business Media, LLC, part of Springer Nature 2024

## Abstract

**Introduction** Bladder cancer is a common malignancy affecting the urinary tract and effective biomarkers and for which monitoring therapeutic interventions have yet to be identified.

**Objectives** Major aim of this work was to perform metabolomic profiling of human bladder cancer and adjacent normal tissue and to evaluate cancer biomarkers.

**Methods** This study utilized nuclear magnetic resonance (NMR) and high-resolution nanoparticle-based laser desorption/ionization mass spectrometry (LDI-MS) methods to investigate polar metabolite profiles in tissue samples from 99 bladder cancer patients.

**Results** Through NMR spectroscopy, six tissue metabolites were identified and quantified as potential indicators of bladder cancer, while LDI-MS allowed detection of 34 compounds which distinguished cancer tissue samples from adjacent normal tissue. Thirteen characteristic tissue metabolites were also found to differentiate bladder cancer tumor grades and thirteen metabolites were correlated with tumor stages. Receiver-operating characteristics analysis showed high predictive power for all three types of metabolomics data, with area under the curve (AUC) values greater than 0.853.

**Conclusion** To date, this is the first study in which bladder human normal tissues adjacent to cancerous tissues are analyzed using both NMR and MS method. These findings suggest that the metabolite markers identified in this study may be useful for the detection and monitoring of bladder cancer stages and grades.

**Keywords** Bladder cancer · Biomarker · Human tissue · Metabolomics · NMR · Laser mass spectrometry

## 1 Introduction

Bladder cancer (BC), also known as urological or urinary bladder cancer, is the tenth most common and thirteenth most deadly cancer globally (sixth in men and seventeenth in women). According to the most recent GLOBOCAN data, BC accounts for approximately 3% of all cancer cases

worldwide. Its prevalence is increasing, particularly in industrialized nations, with around 550,000 new cases diagnosed yearly (Sung et al., 2021). The incidence of bladder cancer rises with age, and the vast majority of cases (80%) occur in those over 65. Moreover, males are four times more likely to be diagnosed with this disease than women (Viswambaram & Hayne, 2020). Environmental and occupational factors are responsible for most cases of bladder cancer, with the most significant risk being associated with tobacco smoke and being responsible for nearly 50% of bladder tumors; smokers are at a 2.5-fold higher risk than nonsmokers (Castelao et al., 2001). Hereditary genetic predisposition causes 7% of cases of bladder cancer (Wong et al., 2018).

The bladder comprises urothelial cells, specialized transitional epithelial cells that collect urine, and smooth muscle that moves and excretes urine via the urethra to the outside. About 90% of BC arises from urothelial cells, mainly in the bladder, but in rare cases, also in the urinary tract (Saginala et al., 2020). This is due to their greater exposure to

✉ Joanna Nizioł  
jnizioł@prz.edu.pl

<sup>1</sup> Department of Urology, John Paul II Hospital, Grunwaldzka 4 St., 36-100 Kolbuszowa, Poland

<sup>2</sup> Faculty of Chemistry, Rzeszów University of Technology, 6 Powstańców Warszawy Ave., 35-959 Rzeszów, Poland

<sup>3</sup> The Department of Chemistry and Biochemistry, Montana State University, Bozeman, MT 59717, USA

<sup>4</sup> Doctoral School of Engineering and Technical Sciences, Rzeszów University of Technology, 8 Powstańców Warszawy Ave., 35-959 Rzeszów, Poland

environmental, potentially mutagenic agents filtered into urine by the kidneys. These tumors have a relatively good prognosis (Mushtaq et al., 2019). The remaining 10% of BC are associated with a much worse prognosis and involve squamous cell carcinoma that affects smooth muscle cells. The World Health Organization classifies superficial bladder tumors as a heterogeneous category that includes urothelial papilloma (a benign lesion), papillary urothelial neoplasm of low malignant potential (PUNLMP), and low- and high-grade papillary malignancy (Montironi & Lopez-Beltran, 2005). Around 75% of patients have non-muscle-invasive bladder cancer (NMIBC) with disease restricted to the mucosa (pTa, Tis) or lamina propria (pT1). The other 25% of newly diagnosed bladder tumors penetrate the muscularis propria bladder wall (pT2), called muscle-invasive bladder cancer (MIBC) (Omar et al., 2019).

One of the first signs of urothelial malignancy is hematuria. It is often detected with a cystoscopy, telescopic endoscopy of the bladder, transabdominal ultrasonography, and/or computer tomography (CT) urography. Individuals with NMIBC are treated by transurethral resection of the bladder tumor (TURBT) and, for high-grade disease, with Bacillus Calmette-Guérin-based intravesical treatment (BCG, modified mycobacterium) (Sahu et al., 2017). While BCG helps delay or prevent the advancement of illness in a subset of individuals, a substantial number of patients ultimately acquire the invasive disease. Additionally, given the current global scarcity of BCG, this group needs alternate, sensitive therapy. Patients with muscle-invasive bladder cancer (MIBC) undergo radical cystectomy and bilateral, regional lymph node dissection, with or without preoperative chemotherapy or chemoradiation. The latest statistics from the American Cancer Society reveal in 2021 that the overall 5-year survival rate for bladder cancer in the United States is roughly 77%. Still, this figure varies significantly depending on the cancer stage at diagnosis (Siegel et al., 2022). If the cancer is localized and has not spread beyond the bladder, the 5-year survival rate is approximately 95%. On the other hand, if the bladder cancer has metastasized and spread to other parts of the body, the 5-year survival rate drops to about 5%. Early detection of cancer enables its resection and improved survival rates.

Despite significant efforts, no clinically viable biomarkers for early detection, diagnosis, or prognosis of BC are currently available. Analyzing the metabolic profiles of tissues and biofluids is a potential strategy for establishing robust small molecule indicators of BC, which would improve our ability to predict cancer progression and evaluate the efficacy of cancer treatment.

Metabolomics is a modern and powerful technology, makes it possible to detect compounds and determine previously unknown mechanisms related to disease progression (Zhang et al., 2020). By examining metabolites in biological

samples such as urine (Jin et al., 2014), serum (Bansal et al., 2013), and tissue (Cheng et al., 2015), metabolomics tracks the metabolic response of living systems to disease or drug toxicity. The information obtained through metabolomic profiling studies on BC can potentially identify valuable biomarkers for diagnostic purposes and as indicators of cancer recurrence (Di Meo et al., 2022a, 2022b).

Over the last two decades, two analytical platforms have been used primarily for metabolomic analysis of diverse kidney cancer samples: mass spectrometry (MS) (Zeki et al., 2020) and nuclear magnetic resonance (NMR) (Emwas et al., 2019). To our knowledge, very few reports are available in the literature regarding human bladder tissue analysis. The first metabolomic profiling of bladder tissues was performed by Putluri et al. (2011) using LC-MS. Analysis of 58 tissues revealed significantly changed levels of 35 mass spectral features within bladder tissues. Further research was carried out in 2013 by Tripathi et al. using the high-resolution magic angle spinning (MAS) NMR method. The findings revealed 22 distinct metabolites in different stages of BC. These results were cross-validated using targeted GC-MS analysis but did not include analysis of normal, unaffected tissues as controls (Tripathi et al., 2013). In a study published in 2017, Piyarathna et al. examined 165 tissues derived from the bladder, including 126 bladder cancer tissues and 39 benign or normal adjacent tissues. Based on UHPLC-HRMS analysis, they found 570 lipids associated with the survival and different clinical stages of BC (Piyarathna et al., 2018).

The present study employed two analytical platforms: NMR and LDI-MS, to investigate the metabolic changes in 198 human tissue samples of 99 BC cancer cases. This work aimed to characterize the most differentiating metabolites between cancer and adjacent normal tissues and also enable the differentiation of cancer stages and grades. The discovery of significant metabolites provides clues at previously poorly understood or unknown metabolic changes that are associated with BC.

## 2 Materials and methods

### 2.1 Materials and equipment

All solvents were of 'LC-MS' grade and purchased from Sigma Aldrich (St. Louis, MO, USA). Deuterium oxide (D<sub>2</sub>O) and DSS (4,4-dimethyl-4-silapentane-1-sulfonic acid) were purchased from Sigma Inc. (Boston, MA, USA).

### 2.2 Collection of human tissue samples

After comprehensive clinical questioning at John Paul II Hospital in Kolbuszowa, tissue samples were gathered

from 99 patients with bladder cancer (20 females, 79 males, average age 72) receiving surgical therapy (Poland). The research was approved by the University of Rzeszow's local Bioethics Committee (Poland, permission number 2018/04/10) and followed all applicable rules and regulations. All the patients in this study were of the Caucasian race. Specimens and clinical data from patients involved in the study were collected with informed consent. All laboratory test results (complete blood count, bleeding profile, kidney function tests, CRP) were within normal ranges. Tissues for the metabolomic study were collected during a transurethral resection of a bladder tumor. For the metabolomic study, we collected roughly cubic fragments of 2–4 mm in size of the cancerous tumor and a fragment of the normal bladder mucosa. A fragment of tumor tissue and normal tissue constituting a control were taken from the same patient. Both of these fragments were cut in half, one part was taken for examination and the other was sent for histopathological examination to verify the diagnosis. Samples were immediately frozen and stored at  $-60^{\circ}\text{C}$  until further use. The pathological and clinical characteristics of the patients are presented in the supplementary material table (Table S1).

### 2.3 Preparation of tissue metabolite extracts

As a result of the extraction of tissue samples, two fractions (phases) were obtained, the upper one containing medium-to-high polarity metabolites and the lower one containing low-polar metabolites. Detailed sample preparation protocols have been described in the Supplementary materials (Section S1) and our recent publication (Nizioł et al., 2021).

### 2.4 Analysis of tissue samples

Tissue extracts were analyzed using high-resolution  $^1\text{H}$  NMR (upper phase) and silver-109 nanoparticle-based laser desorption/ionization mass spectrometry ( $^{109}\text{AgNPs}$ -LDI-MS, upper and lower phase, analyzed separately). Silver-109 nanoparticles ( $^{109}\text{AgNPs}$ ) were generated with pulsed fiber laser (PFL) 2D galvoscaner (2D GS) laser synthesis in solution/suspension (LASiS) as described in our previous publication (Płaza et al., 2021). Supplementary data detail the acquisition and processing of NMR and MS spectra (S2–S4).

### 2.5 Multivariate statistical analysis

MetaboAnalyst version 5.0 online software was used to analyze all metabolite datasets (Pang et al., 2021). The multivariate statistical analysis used here is similar to the one described in our recent publications (Nizioł et al., 2021, 2022; Ossoliński et al., 2022). Briefly, the metabolite data obtained from each analytical technique

was log-transformed, auto-scaled, and normalized on the weight of the fresh tissue. The resulting metabolite profiles were then subjected to unsupervised Principal Component Analysis (PCA) and Orthogonal Partial Least Squares Discriminant Analysis (OPLS-DA). Metabolites which Variable Importance in Projection (VIP) values, associated with the OPLS-DA modeling, were greater than 1.0 were considered potentially significant discriminators of BC tissues from adjacent normal tissue. Permutation tests using 2000 steps were used to validate and assess the accuracy of the OPLS-DA models. A paired parametric t-test with Mann–Whitney and Bonferroni correction and fold change (FC) analysis were employed to evaluate the statistical significance of tissue metabolite level differences. Metabolites with FDR corrected  $P$ -values and false discovery rates (FDR) less than 0.05 and  $\text{FC} > 2$  or  $< 0.5$  were considered statistically significant (Benjamini et al., 2001). Furthermore, receiver operating characteristic curve (ROC) analyses were performed with random forest modeling to validate the OPLS-DA models and assess the metabolites' diagnostic value. Mass features identified by NMR and MS, respectively. Metabolite variables with an AUC (area under the curve) greater than 0.75 were deemed relevant to the discrimination of BC versus AN tissue metabolome. Training and validation metabolite datasets were subjected to independent multivariate statistical analyses. Compounds that separated BC tissues from adjacent normal tissues were chosen for external validation, which employed two independent datasets (here referred to as the training and validation datasets) to evaluate the performance of the OPLS-DA models (Ho et al., 2020). The established statistical criteria were applied to both training and validation datasets. A metabolic pathway impact analysis was performed using MetaboAnalyst 5.0 (Pang et al., 2021) and the Kyoto Encyclopedia of Genes and Genomes (Okuda et al., 2008) to identify metabolic pathways that are, in all likelihood, impacted by bladder cancer. To determine whether there were significant disparities in the average math test scores between different stages and grades of BC, we carried out a one-way analysis of variance (ANOVA) with Tukey's post-hoc testing.

## 3 Results

To uncover possible discriminant biomarkers of bladder cancer, 198 metabolite extracts from frozen bladder tissue samples (99 BC and 99 AN – 'adjacent normal') were examined using high-resolution 1D  $^1\text{H}$  NMR and silver-109 nanoparticle-based laser desorption/ionization mass spectrometry ( $^{109}\text{AgNPs}$ -LDI-MS).

### 3.1 Distinguishing between bladder cancer and normal tissues by $^1\text{H}$ NMR metabolomics

In total, 43 metabolites were identified and quantified in each tissue sample using  $^1\text{H}$  NMR spectroscopy following published protocols (Nizioł et al., 2021). Figure 1 depicts an overlay of NMR spectra of cancer and normal tissue samples. Detailed spectra analysis revealed significant differences in metabolite levels between BC and AN tissues.

In the next stage of our study, we implemented external validation by dividing our data into two distinct subsets in order to bolster the robustness and credibility of our results. NMR datasets were divided into two subsets: a training data set to train a model ( $n=69$  BC and  $n=69$  AN) and a validation data set ( $n=30$  BC and  $n=30$  AN). Both sets were matched in terms of cancer grade and stage as well as age and gender. We utilized the training set to identify potential biomarkers. Subsequently, the independent validation set was employed to confirm these findings. This was crucial in mitigating the risk of overfitting our data to the specific sample group, thereby enhancing the likelihood that our results would be applicable to a broader population. Metabolite

concentrations from both groups were statistically analyzed to assess whether differences in metabolite levels between cancer and normal tissue were significant. Findings from this analysis are reported in supplementary data Tables S2 and S3. Unsupervised score plots using PCA were generated for both subsets, revealing a poor distinction between BC and AN tissue. The most distinct separation between groups was identified using the first and second principal components, PC1 and PC2, which accounted for 48.8% and 10.0% of the variation in the training set, as shown in Fig. 2a. Similarly, in the validation set, a noticeable separation was observed between cancer and normal tissue samples along the first and second components, which accounted for 52.3% and 11.9%, respectively.

Subsequently, a supervised multivariate analysis was performed to investigate the metabolic distinctions between the BC and AN groups in both the training and validation sets, using OPLS-DA analysis. As depicted in Fig. 2b for the training set, and Fig. S1b in the supplementary data for the validation set, a distinct separation was observed between the two groups in the score plot. To confirm the reliability of the OPLS-DA model, two thousand permutation tests were

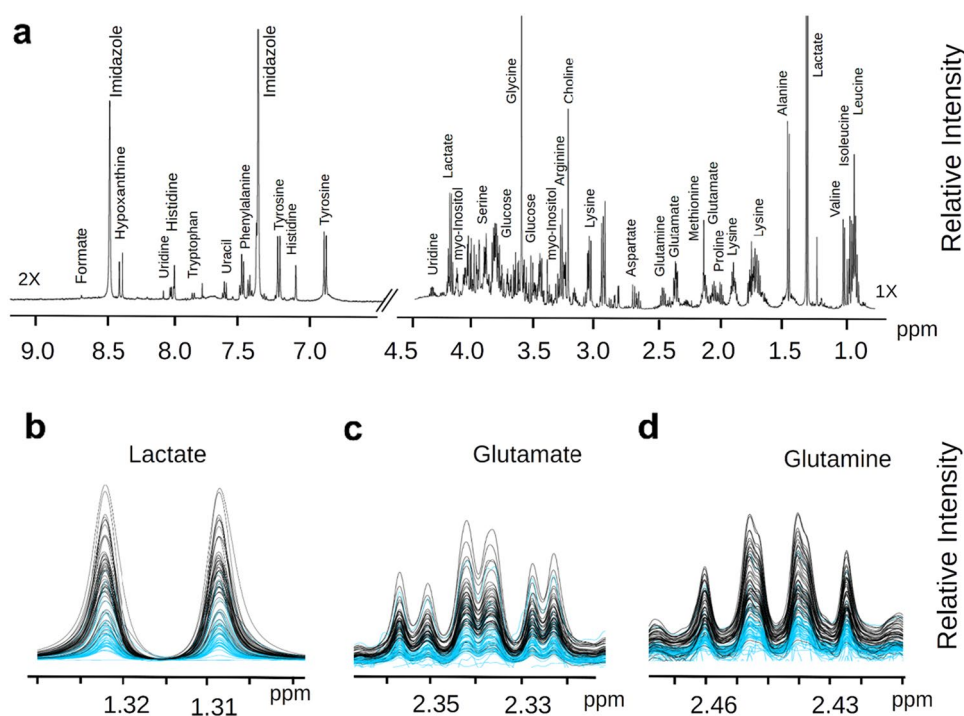


**Fig. 1** Representative 1D  $^1\text{H}$ -NMR spectra of metabolites extracts obtained from cancerous versus healthy tissue of bladder cancer (BC) patients. **a** Full 1D  $^1\text{H}$  NMR spectrum of a bladder cancer (BC) patient metabolite sample recorded on MSU 600 MHz (14 T) solution NMR spectrometer. The chemical shift locations of several identified metabolites in the tissue metabolite extracts of BC tissue compared to AN tissue are labeled. Panels **b–d** depict the overlays of  $^1\text{H}$  NMR spectra from BC tissue samples (black) and AN tissue samples (blue).

Expanded regions of the spectra are shown in **(b)** for the chemical shift region 1.33–1.30 ppm corresponding to lactate; **(c)** for the chemical shift region 2.37–2.31 ppm corresponding to glutamate; and **(d)** for the chemical shift region 2.48–2.41 ppm corresponding to glutamine. The weight-normalized spectral overlays clearly indicate that the levels of these metabolites are higher in the cancer tissue of the BC compared to the levels found in the healthy tissue controls

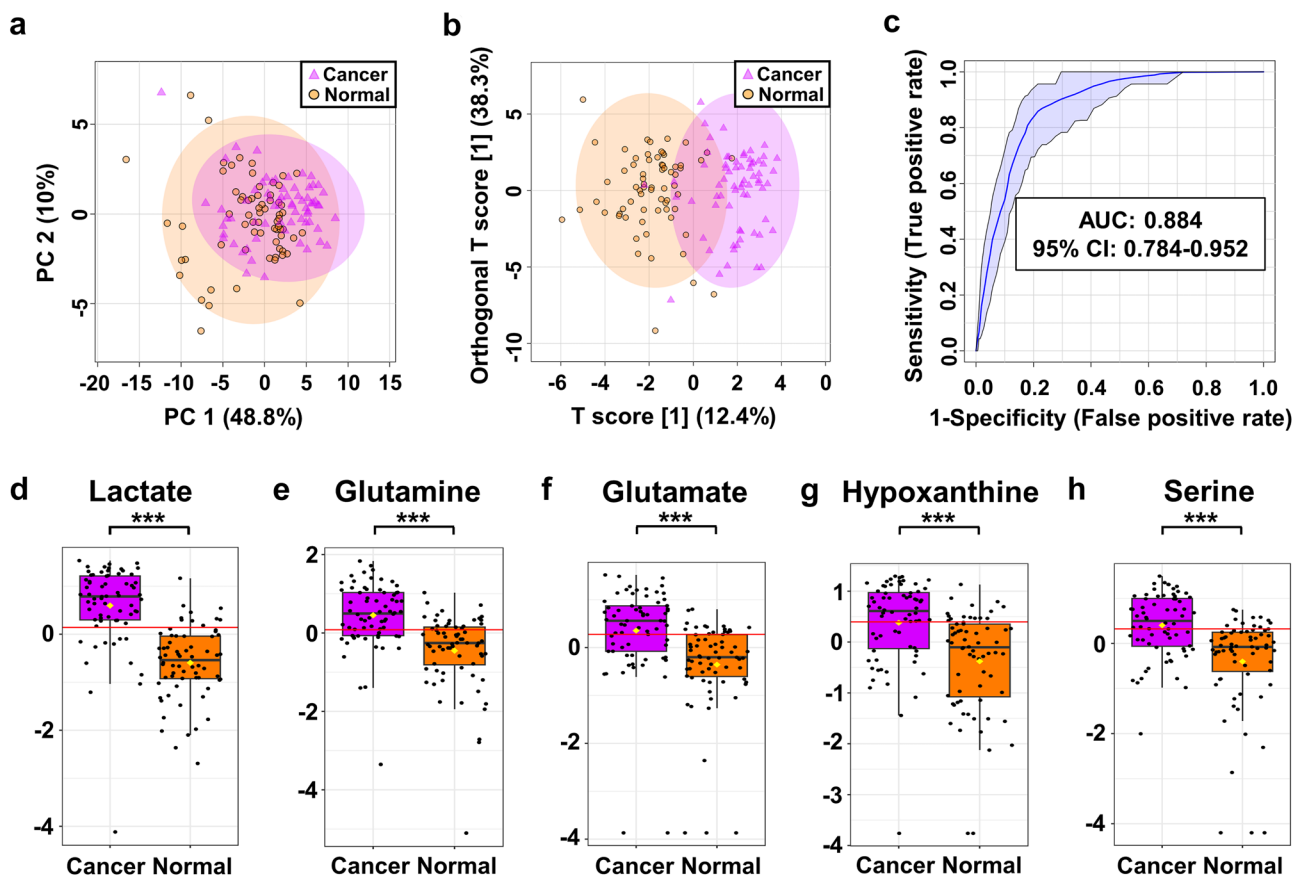


**Fig. 2** Cancer and normal tissue metabolite profiles obtained from  $^1\text{H}$  NMR data distinguish BC and AN samples in the training set. The tumor (violet) and normal (orange) tissue samples were evaluated using **a** 2D PCA, and **b** OPLS-DA scores. **c** ROC curves of six dis-

tinct metabolites: lactate, glutamine, glutamate, hypoxanthine, serine, and threonine. **d–h** Box-whisker plots of selected metabolite levels in samples from BC and AN tissue. *AUC* area under the curve, *PC* primary component, *ROC* the receiver operator characteristic

conducted, and the statistical robustness of the model was verified, as shown in Table S4 in supplementary data. In the training set, there was good discrimination between the two groups ( $Q^2=0.536$ ,  $R^2Y=0.682$ ,  $P$ -value  $< 5E-04$  (0/2000)), revealing substantial differences in the metabolic profiles of BC vs AN tissues sample. The permutation test supported the group separations found with OPLS-DA in the validation set ( $Q^2=0.287$ ,  $R^2Y=0.466$ ,  $P$ -value  $< 5E-04$  (0/2000)).

To evaluate the diagnostic performance of the OPLS-DA models and to identify potential tissue polar metabolite biomarkers of bladder cancer, ROC analysis was conducted on both the training and validation datasets, along with the examination of VIP plots resulting from the OPLS-DA modeling. The paired parametric t-test with Mann–Whitney and Bonferroni correction was employed to investigate the statistical significance of metabolite level differences. A combined analysis of VIP scores ( $> 1.0$ ), t-tests (FDR corrected  $P$ -values  $< 0.05$ ), fold change ( $FC > 2.0$  or  $< 0.5$ ), and AUC ( $> 0.75$ ) of training and validation set metabolite data identified six tissue metabolites as significant discriminators of BC versus

AN tissue, as presented in Table 1. These included lactate, glutamine, glutamate, hypoxanthine, serine, and threonine.

ROC studies and random forest modeling were performed to determine the diagnostic value of the six identified metabolites. The classification ROC model (as shown in Fig. 2c and Supplementary Fig. S1c) demonstrated that the combination of the differential levels of these six metabolites was a reliable discriminator in both data sets, with an AUC of over 0.853. The validity of the ROC model was confirmed by a permutation test with 1000 permutation steps resulting in a  $p$ -value below 0.001. The highest significance in the training set, with an AUC of over 0.80, was achieved for two metabolites: lactate (AUC = 0.889, specificity = 82%, and sensitivity = 85%), and glutamine (AUC = 0.800, specificity = 72%, and sensitivity = 71%). Box and whisker plots for selected metabolites are presented in Fig. 2d–h. Table 1 summarizes the most important statistical parameters for these five metabolites identified by  $^1\text{H}$  NMR as potential biomarkers of BC. These findings suggest that these six metabolites may

**Table 1** Results of targeted quantitative study of potential BC biomarkers derived from  $^1\text{H}$  NMR data of tissue samples (P value 0.05; VIP > 1.0; FC > 2.0 or < 0.5)

Metabolite		VIP <sup>a</sup>	P value <sup>b</sup>	FDR <sup>b</sup>	FC <sup>c</sup>	AUC	Spec. [%] <sup>d</sup>	Sens. [%] <sup>d</sup>
Lactate	Cancer vs. normal	2.02	2.81E-10	1.21E-08	3.832	0.889	82	85
Glutamine		1.59	3.62E-08	2.59E-07	2.296	0.800	72	71
Glutamate		1.23	7.96E-08	4.28E-07	2.132	0.780	65	75
Hypoxanthine		1.39	7.87E-09	1.13E-07	2.109	0.754	65	78
Serine		1.31	1.30E-08	1.20E-07	2.625	0.753	59	84
Threonine		1.29	1.40E-08	1.20E-07	3.246	0.751	57	82
Lactate	HG BC vs. HG AN	2.45	5.16E-05	2.22E-03	3.780	0.864	88	77
Ethanolamine		1.54	3.64E-04	5.21E-03	2.285	0.714	69	73
Lactate	LG BC vs. LG AN	1.75	6.34E-09	9.09E-08	4.341	0.922	88	91
Alanine		1.44	1.17E-06	6.28E-06	2.553	0.801	67	79
Choline		1.43	6.35E-05	1.37E-04	2.014	0.779	77	72
Glutamine		1.49	1.35E-07	8.29E-07	2.807	0.870	79	77
Hypoxanthine		1.31	4.94E-09	9.09E-08	2.309	0.816	74	77
Leucine		1.18	1.62E-06	7.75E-06	2.594	0.759	65	86
Methionine		1.42	2.26E-09	9.09E-08	4.348	0.812	72	84
Phenylalanine		1.22	2.30E-08	2.47E-07	3.647	0.764	63	79
Serine		1.44	1.00E-07	7.95E-07	2.725	0.817	74	77
Threonine		1.40	1.11E-07	7.95E-07	2.888	0.789	60	91
Tyrosine		1.25	3.57E-06	1.53E-05	2.791	0.759	74	77
Lactate	pTa BC vs. pTa AN	1.84	2.57E-10	3.69E-09	4.560	0.928	88	86
Glutamine		1.68	1.77E-09	1.52E-08	2.747	0.884	80	80
Serine		1.28	2.89E-09	2.07E-08	2.753	0.814	69	90
Hypoxanthine		1.32	1.43E-10	3.07E-09	2.334	0.809	65	88
Alanine		1.40	5.23E-08	2.81E-07	2.498	0.805	69	80
Methionine		1.35	8.76E-11	3.07E-09	4.140	0.804	71	86
Threonine		1.32	1.18E-09	1.27E-08	2.758	0.798	63	88
Choline		1.52	5.46E-06	1.24E-05	2.021	0.793	74	76
Aspartate		1.12	2.34E-06	6.69E-06	2.824	0.786	67	82
Ethanolamine		1.15	8.35E-07	2.76E-06	2.238	0.770	71	76
Phenylalanine		1.03	4.65E-09	2.86E-08	3.621	0.761	61	90
Tyrosine		1.13	7.30E-07	2.62E-06	2.599	0.755	71	82
Trimethylamine	pT1 BC vs. pT1 AN	2.09	9.65E-04	2.08E-02	0.429	0.832	84	58
Lactate		2.40	7.25E-05	3.12E-03	3.760	0.859	74	68

AN adjacent normal, AUC area under the curve, BC bladder cancer, FC fold change, FDR false discovery rate, HG high-grade, LG low-grade, pT1 and pTa high risk non-muscle invasive bladder cancer, pT2 muscle invasive bladder cancer, VIP variable importance in projection scores

<sup>a</sup>VIP scores derived from OPLS-DA model

<sup>b</sup>FDR corrected P value and FDR determined from Student's *t*-test

<sup>c</sup>Fold change between BC and AN tissues calculated from the concentration mean values for each group—cancer-to-normal ratio

<sup>d</sup>ROC curve analysis for individual biomarkers

have enhanced diagnostic potential and could be valuable indicators of malignant versus normal tissues of patients with bladder cancer when evaluated together.

### 3.2 Distinguishing between grades of bladder cancer and normal tissues based on $^1\text{H}$ NMR metabolite profiling analysis

To assess the potential of  $^1\text{H}$  NMR metabolite profiles of tissue extracts to differentiate between different grades of BC and AN tissue, we performed PCA, OPLS-DA, and one-way ANOVA analysis on training and validation data

sets. The analysis included 94 tissue samples from patients with high-grade (HG) and low-grade (LG) cancer, with three samples from a papillary urothelial neoplasm of low malignant potential (PUNLMP) patients excluded. The training data set ( $n=26$  HG BC and HG AN and  $n=43$  LG BC and AN) was used to train the PCA model. The validation data set ( $n=11$  HG BC and AN and  $n=15$  LG BC and AN) was used to verify the validity and robustness of the separate group clustering observed in the PCA model. In both the training and validation sets, PCA and OPLS-DA scores plots showed good separation between HG BC and HG AN tissue (Figs. 3a, b, S2a, b in supplementary material).

In the HG BC vs. HG AN tissue OPLS-DA model, two metabolites, including lactate and ethanolamine, were considered significant ( $VIP > 1$ ,  $P$ -value,  $FDR < 0.05$ ,  $FC < 0.5$  or  $> 2.0$ ,  $AUC > 0.70$ ) in both the training and validation sets (Table 1). The ROC model for classification (Fig. 3C) indicated that the collective concentrations of these two metabolites were a dependable differentiator with an AUC of 0.851. These compounds were found in significantly higher concentrations in the cancer tissue compared to the adjacent normal tissue. Analysis of LG BC vs. LG AN in the training and validation sets of the OPLS-DA model showed that eleven commonly identified compounds were important in separating the two groups (Table 1). PCA and OPLS-DA scores plots resulting from this analysis illustrate the extent of the separation of LG BC from LG AN based on differential tissue metabolite profiles in the training and validation datasets (Figs. 3d, e and S3a, b in supplementary data). Based on the results of univariate ROC curve analyses, we determined that these models have satisfactory diagnostic performance with  $AUC = 0.911$  (Fig. 3f). Although PCA analysis was unable to separate the groups based on distinct tumor grades (data not shown), the cancer groups separated clearly from the AN group.

### 3.3 Distinguishing between stages of bladder cancer and normal tissues based on $^1\text{H-NMR}$ metabolite profiling

A  $^1\text{H}$  NMR metabolomics study of tissue samples was also employed to evaluate whether unique metabolite patterns can help distinguish between stages of BC. We performed PCA, OPLS-DA, and non-parametric one-way ANOVA analyses on a total of 198 tissue extracts from 70 patients with pTa BC, 19 patients with pT1 BC, and 12 patients with pT2 BC. Due to insufficient patients with pT1 and pT2 malignancy, validation on a separate dataset was performed only for samples from patients with pTa BC. A training data set was created with  $n=49$  pTa BC and  $n=49$  AN tissue extracts. A validation data set was made with  $n=21$  pTa BC, and  $n=21$  AN tissue extracts.

The PCA and OPLS-DA score plots demonstrated a small but distinctive separation between normal and cancer tissue samples from patients with pTa stages of BC (Fig. 4a, b). The performance of this model was then evaluated using ROC analysis. The AUC value of 0.921 in the training set indicated very good classification and suggested that the model has a high probability of correctly classifying the samples with pTa BC and can be considered an effective classification tool (Fig. 4c).

The score plots generated by PCA and OPLS-DA indicated a noticeable distinction between the cancerous and non-cancerous tissue samples obtained from patients diagnosed with pT1 stage BC (Fig. 4d, e). From the ROC plot (Fig. 4f), it can be seen that this model also provided a very high classification ability with an AUC value of 0.946). Based on the cut-off criteria ( $FC > 2$  or  $< 0.5$ ,  $VIP > 1$ ;  $AUC > 0.75$ ,  $P$ -value and  $FDR < 0.05$ ), finally, 12, and 2 metabolites appeared to be most relevant for sample distinction between pTa BC vs. AN, and pT1 BC vs. AN, respectively (Table 1). Unfortunately, in the case of tissue extracts from patients with stage pT2, obtaining a significant separation of cancer and regular groups was impossible. Also, comparing the three cancer stage groups (pT1 versus pTa versus pT2) revealed no statistically significant differences (data not shown).

### 3.4 Untargeted metabolic profiling of tissue using PFL-2D GS LASiS $^{109}\text{AgNPs}$ LDI-MS

Pulsed fiber laser ablation synthesis was employed to generate silver-109 nanoparticles in solution (PFL-2D GS LASiS  $^{109}\text{AgNPs}$ ). These nanoparticles were then utilized for laser mass spectrometry-based profiling of BC and AN extracts. We analyzed the bladder tissue's polar and non-polar metabolite extracts separately and randomly divided the data into two subsets for statistical analysis. The training dataset included 69 bladder cancer (BC) and 69 normal (AN) tissue samples, while the validation dataset included 30 BC and 30 AN tissue samples. 355 and 299 common features were detected in the polar and non-polar extracts of tissue samples, respectively.

2D-PCA and OPLS-DA scores plots were generated from multivariate statistical analysis of the PFL-2D GS LASiS  $^{109}\text{AgNPs}$  LDI-MS mass spectral features obtained from polar tissue extracts. These plots clearly distinguished the cancerous tissue from the normal tissue as a result of their distinct metabolite profiles, as shown in the Supplementary data (Fig. S4). For the training dataset, the validation of the OPLS-DA model using 2000 permutations resulted in  $R^2Y$  and  $Q^2$  values of 0.872 ( $P$  value  $< 5E04$ ) and 0.964 ( $P$  value  $< 5E04$ ) (Table S4, supplementary data), while  $R^2Y$  and  $Q^2$  values of 0.807 ( $P$  value  $< 5E04$ ) and 0.983 ( $P$  value  $< 5E04$ ), respectively, were measured when analyzing

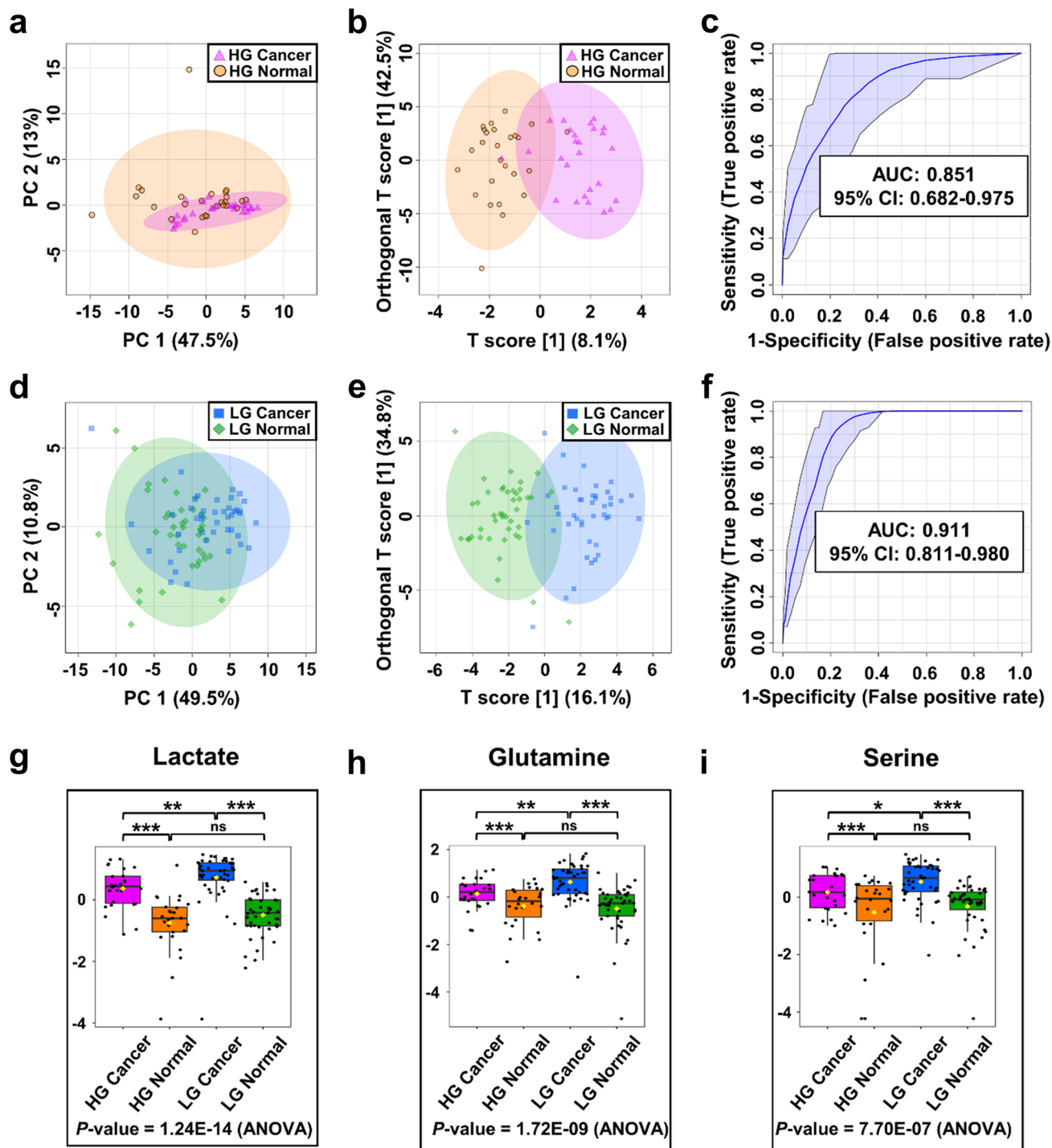


**Fig. 3** Analysis of the tissue metabolite profiles obtained from the <sup>1</sup>H NMR training dataset and assessment of whether metabolite differences can be used to differentiate between various grades of bladder cancer and normal tissue samples. **a** PCA and **b** OPLS-DA score plots of HG BC (violet) and AN (orange) tissue samples. **c** ROC curves of the two most differentiating HG BC metabolites. **d** PCA and **e** OPLS-DA score plots of LG BC (blue) and AN (green)

tissue samples. **f** ROC curves of the eleven most differentiating LG BC metabolites. **g-i** The box-and-whisker plots of selected metabolites were observed in the control, HG, and LG BC tissue samples. AN adjacent normal, AUC area under the curve, HG high grade, LG low grade, PC primary component, ROC the receiver operator characteristic;

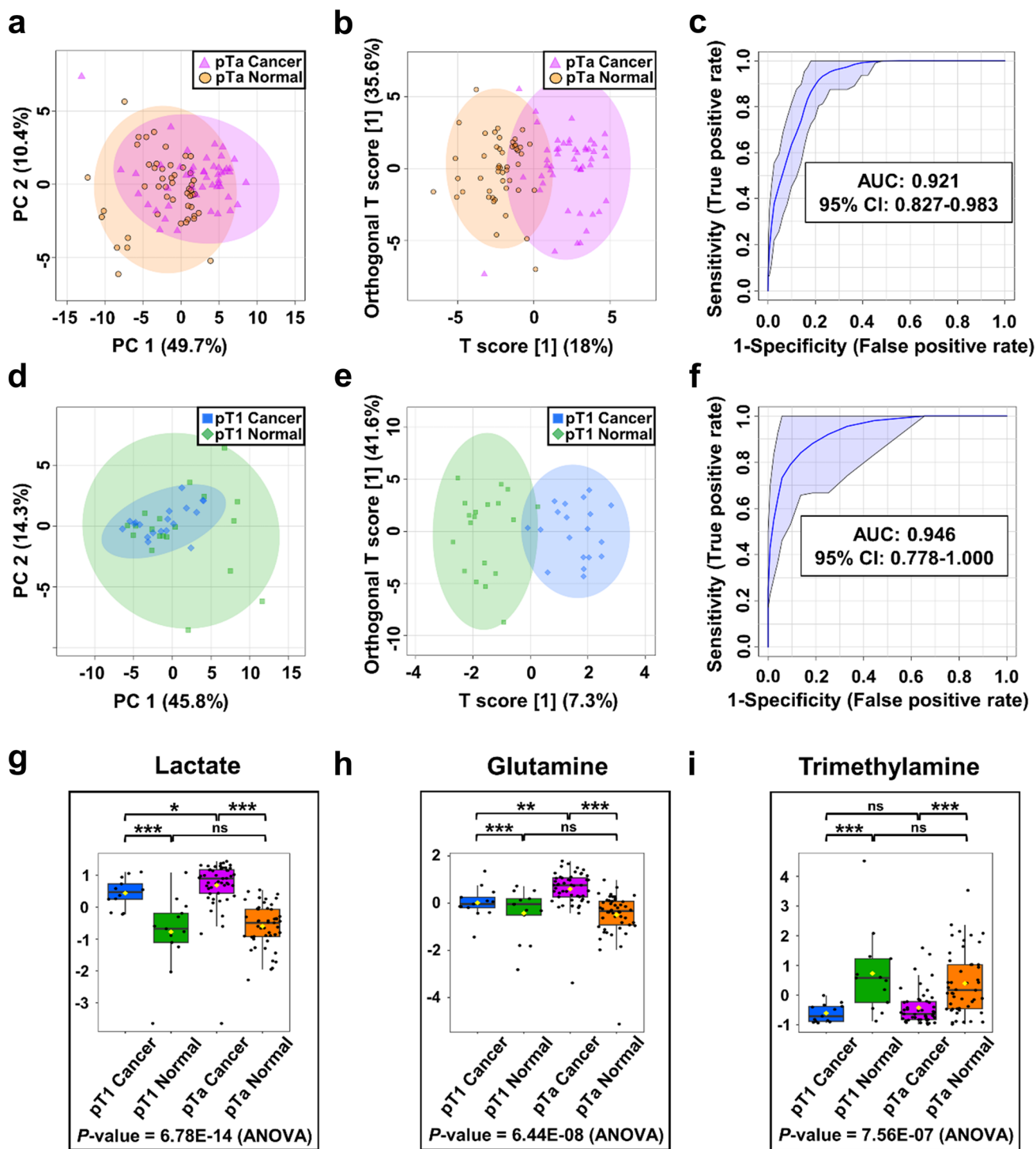


**Fig. 4** Analysis of the tissue metabolite profiles obtained from the <sup>1</sup>H NMR training dataset and assessment of whether metabolite differences can be used to differentiate between various stages of bladder cancer and normal tissue samples. **a** PCA and **b** OPLS-DA score plots of pTa BC (violet) and AN (orange) tissue samples. **c** ROC

curves of the twelve most differentiating pTa BC metabolites. **d** PCA and **e** OPLS-DA score plots of pT1 BC (blue) and AN (green) tissue samples. **f** ROC curves of the two most differentiating pT1 BC metabolites. AN adjacent normal, AUC area under the curve, PC primary component, ROC the receiver operator characteristic

the MS metabolomics data present in the validation dataset. This analysis was followed by univariate and multivariate ROC analysis for both training and validation datasets (Fig. S4, supplementary data). Supplementary data Fig. S4 provides a summary of all ROC curves generated from the analysis of the training and validation datasets, with a range of feature counts (i.e., 5, 10, 15, 25, 50, and 100), along with corresponding AUC values and confidence intervals. Notably, the 50-feature panel of model 5 in the training set and the 25-feature panel of model 4 in the validation set exhibited excellent discrimination power for BC diagnosis ( $AUC > 0.971$ ), as illustrated in supplementary Fig. S4. Based on the cut-off criteria ( $FC > 2$  or  $< 0.5$ ,  $VIP > 1$ ;  $AUC > 0.75$ ,  $P$  value and  $FDR < 0.05$ ), finally, 97  $m/z$  values appeared to be most relevant for sample distinction between cancer and normal tissue in both training and the validation datasets.

The mass spectral features obtained from non-polar tissue extracts generated from untargeted PFL-2D GS LASiS  $^{109}\text{AgNPs}$  LDI-MS experiments were also analyzed using PCA and OPLS-DA to identify the mass spectral features that most differentiated BC from AN tissue extracts from patients with BC, using both training and validation datasets (Fig. S5, supplementary data). The results of both PCA and OPLS-DA scores plots indicate a clear separation between cancer and normal groups in both the training and validation data subsets. This suggests that PFL-2D GS LASiS  $^{109}\text{AgNPs}$  LDI-MS-based metabolite profiling of non-polar tissue extracts is an effective method for identifying characteristic metabolic differences that distinguish BC from AN groups. The OPLS-DA model was validated using 2000 random permutation steps, which resulted in  $R^2Y$  and  $Q^2$  values of 0.773 ( $P$  value  $< 5 \text{E}04$ ) and 0.898 ( $P$  value  $< 5\text{E}04$ ), respectively, for the training dataset. Similarly, for the validation dataset,  $R^2Y$  and  $Q^2$  values of 0.730 ( $P$  value  $< 5\text{E}04$ ) and 0.971 ( $P$  value  $< 5\text{E}04$ ) were obtained (see Supplementary data, Table S4). Following the completion of the analysis, both univariate and multivariate ROC analyses were performed. Supplementary Fig. S5 summarizes all the ROC curves generated from the training and validation datasets, with a range of feature counts (i.e., five, ten, fifteen, twenty-five, fifty, and one hundred), along with corresponding AUC values and confidence intervals for each curve. The 15-feature panel of model 3 in the training dataset demonstrated the highest accuracy, while the 10-feature panel of model 2 in the validation dataset exhibited the highest accuracy. In both the training and validation sets, a total of 36 spectral features were identified in non-polar tissue extracts with VIP scores  $> 1.0$ , FDR-corrected  $P$ -value  $< 0.05$ ,  $FC < 0.5$  or  $> 2.0$ , and  $AUC > 0.75$ .

Subsequently, selected mass spectral features observed in the PFL-2D GS LASiS  $^{109}\text{AgNPs}$  LDI-MS spectra of polar and non-polar tissue extracts were subjected to

putative compound identification. This was accomplished by searching against various metabolite databases, including the Human Metabolome Database (HMDB) (Wishart et al., 2007), the MetaCyc Metabolic Pathway Database (Caspi et al., 2018), and the LIPID MAPS® Lipidomics Gateway (Sud et al., 2007). By comparing the spectral features observed in PFL-2D GS LASiS  $^{109}\text{AgNPs}$  LDI-MS mass spectra with those of compounds present in the aforementioned databases, a total of 30 and 4 mass spectral features from polar and non-polar tissue extracts respectively were assigned putative metabolite IDs. Detailed information on these identified features is provided in Supplementary data Table S5.

## 4 Discussion

In this study, we performed targeted and untargeted metabolic profiling of tissues obtained from patients diagnosed with BC. The control tissue was sourced from the same patient as the cancerous tissue which helped in comparing the cancerous and non-cancerous states more accurately, as it accounts for individual variability. Due to the availability of tissue samples, this approach is very rarely used, especially in the case of bladder cancer. Our objective was to generate distinctive metabolic signatures that could aid in the early and accurate detection of BC using NMR and  $^{109}\text{AgNPs}$  LDI-MS techniques. We performed targeted  $^1\text{H}$  NMR analysis of normal and neoplastic tissues to identify a panel of 43 metabolites. Thirty-four of these compounds were present in higher concentrations and nine at lower concentrations in the cancer tissue compared to adjacent normal ones (see Tables S2, 3 in Supplementary data). The elevated levels of these 34 metabolites may indicate an increased synthesis of tumor-related metabolites that are secreted by cancer cells or changes in the composition of non-cancerous tissues caused by tumor infiltration through the epithelial barrier. In addition, the presence of tumors may trigger inflammatory responses that contribute to the elevation of certain metabolites. The metabolomics data obtained through  $^1\text{H}$  NMR analysis showed that six compounds exhibited higher concentrations in cancerous tissue than in normal tissue, and these compounds effectively differentiated between the two groups with significant discriminating power (Table 1). These included lactate, glutamine, glutamate, hypoxanthine, serine, and threonine.

Among the metabolites that effectively discriminated between cancerous and normal tissue samples, lactate emerged as a particularly significant biomolecule with a high VIP value. As the anion of a hydroxy carboxylic acid, lactate plays a key role in human metabolism and serves as a crucial energy reservoir (Rosenstein et al., 2018). By enabling the maintenance of ATP production and mitigating acidosis

caused by ATP hydrolysis, lactate plays a vital function in cellular metabolism (Rosenstein et al., 2018). Furthermore, lactate has been identified as a significant contributor to acidosis in the tumor microenvironment (TME), which is associated with an acid-resistant phenotype that enables cancer cells to promote their survival (Afonso et al., 2020). In normal mammalian cells, glucose is metabolized to pyruvate, which enters the tricarboxylic acid (TCA) cycle within the mitochondria, leading to the production of a substantial amount of ATP through oxidative phosphorylation. Under low oxygen conditions, cells can switch to lactate metabolism, converting pyruvate to lactate and yielding only two ATP molecules per glucose molecule. However, cancer cells influenced by genetic and molecular changes including alterations in the VHL/HIF- $\alpha$  pathway, undergo a fundamental metabolic reprogramming (Massari et al., 2016). This shift, known as the Warburg effect (Warburg, 1956) enables cancer cells to preferentially utilize glycolysis over mitochondrial respiration for energy production, even in the presence of oxygen, resulting in increased lactate production (Lucarelli et al., 2019). The Warburg effect is not merely a method for energy production, it is intricately linked with the uncontrolled growth and proliferation of cancer cells, including those in urothelial carcinoma. A high glycolytic flux in these cells is sustained by the overexpression of glycolysis-related genes, leading to excess production of pyruvate, alanine, and lactate (Bianchi et al., 2017; di Meo et al., 2022a, 2022b; Lucarelli et al., 2015, 2018, 2022). This overproduction of lactate contributes to the acidification of the tumor microenvironment, which can promote carcinogenesis, extracellular matrix degradation, and enhance the invasiveness of cancer cells (Gatenby et al., 2006). Moreover, lactate has been implicated in promoting metastasis and contributing to resistance against chemo-radiotherapy, making it a focal point in cancer research (Fischer et al., 2007). The clinical relevance of these metabolic alterations is underscored by the potential of lactate as a biomarker for cancer diagnosis and prognosis. Studies have consistently found elevated lactate levels in the cancer tissues of patients with bladder cancer compared to normal tissues (Liu et al., 2016; Massari et al., 2016; Ragone et al., 2016). This is supported by analyses of urine and serum samples from bladder cancer patients using techniques such as NMR and LC-MS, which have confirmed these findings (Bansal et al., 2013; Tripathi et al., 2013; Wittmann et al., 2014). The consistent detection of higher lactate levels in tumor samples suggests that lactate could serve as a promising biomarker for the diagnosis and monitoring of bladder cancer, providing a non-invasive means to assess the disease state and response to treatment.

Glutamine and glutamate stand out as key differentiators between cancerous and normal bladder tissues, exhibiting the highest variable importance in projection (VIP) value among metabolites. As one of the most abundant

free amino acids, glutamine is integral for nitrogen transport and acid-base balance in the body (Hall et al., 1996). It serves as a primary energy source for rapidly dividing cells, including cancer cells, and is involved in the excretion of nitrogen compounds (Labow & Souba, 2000). Glutamate is also a fundamental metabolite in the human body derived from alpha-amino acid anions and is the conjugate base of glutamic acid. It contains anionic carboxyl groups and a cationic amino group and plays a crucial role in both normal and abnormal brain functioning, as well as in peripheral organs (Danbolt, 2001). Cancer cells, including those in bladder cancer, exhibit a high demand for glutamine due to its role in supporting anabolic processes necessary for rapid cell growth (Guin et al., 2014). These cells upregulate glutaminolysis, where glutamine is metabolized into glutamate and then into alpha-ketoglutarate ( $\alpha$ -KG), which enters the TCA cycle. This metabolic adaptation not only provides energy but also supplies building blocks for the synthesis of nucleotides and amino acids. The increased activity of glutaminolysis in cancer cells leads to elevated levels of glutamine and glutamate, which are critical for tumor growth and survival. Changes detected in the concentrations of amino acids such as glutamine and glutamate, which feed into the Krebs cycle through glutaminolysis, indicate a metabolic pattern that may coincide with increased glutaminolytic activity (Lucarelli et al., 2018). However, the mechanisms and effects of glutamine metabolism in cancer are still being actively researched (Sun et al., 2019). More recently, further studies have provided knowledge of the potential use of glutamine and glutamate as biomarkers for bladder cancer (Cheng et al., 2015; Loras et al., 2019a).

Our findings, which demonstrate elevated levels of glutamine and glutamate in tumor tissue, are in line with numerous prior studies that have revealed a significant increase in glutamine levels in serum and urine samples from bladder cancer patients in comparison to controls (Bansal et al., 2013; Wittmann et al., 2014). Moreover, a previous NMR-based study of bladder cancer tissue also reported higher glutamine levels in tumor tissue relative to benign disease (Tripathi et al., 2013). Furthermore, in time series metabolomics analyses of urine and serum samples obtained from bladder cancer patients pre- and post-resection, glutamine demonstrated significant potential in differentiating neoplastic samples from healthy ones (Gupta et al., 2020; Jacyna et al., 2022). Similar results have been obtained in other urinary tract cancers such as kidney cancer. Interestingly, of all the amino acids tested, almost all were significantly reduced in cancer tissue, except glutamine, glutamate, and cysteine, which were significantly increased in tumors. Cancer cells with defective mitochondria use glutamine-dependent reductive carboxylation rather than oxidative metabolism as the major pathway of citrate formation (Lucarelli et al., 2022).

Hypoxanthine is a natural purine base that is produced during purine degradation and can be converted to xanthine and uric acid while generating reactive oxygen species through the action of the xanthine oxidase enzyme (Lawal & Adeloju, 2012). Due to its diminutive and polar structure, hypoxanthine can easily accumulate in biological fluids and tissues, making it a potential indicator for medical diagnosis (Garg et al., 2022). Specifically, hypoxanthine is a significant product that is generated during the breakdown of nucleotides and can serve as a precursor of uric acid and is an intermediate in the breakdown of purines (Pasikanti et al., 2010). As such, its quantification is highly valuable for relevant clinical diagnoses (Dervisevic et al., 2016). Furthermore, increased levels of hypoxanthine are associated with decreased levels of uric acid, adenosine, and inosinic acid. In cancer cells, this pathway is often disrupted, leading to the accumulation of hypoxanthine. Therefore, the measurement of hypoxanthine levels can not only serve as a potential biomarker for medical diagnosis but may also provide important information about the underlying metabolic changes in cancer cells (Rodrigues et al., 2016). In our studies, hypoxanthine levels were higher in cancer tissue compared to normal. This compound has also been previously detected in higher amounts in the urine and serum of BC patients and suggested to be a potential bladder cancer biomarker (Alberice et al., 2013; Gao et al., 2012; Hu et al., 2021; Loras et al., 2018; Tan et al., 2017; Wittmann et al., 2014).

Serine and threonine are amino acids that were also found to be in high concentrations in BC tissue compared to normal in our study. Serine is an endogenous amino acid that plays a significant role in various biosynthetic pathways in the human body, such as pyrimidine, purine, creatine, and porphyrin biosynthesis. Cancer cells utilize serine as the primary source of one-carbon units, which are necessary for the production of cellular components and proliferation (Newman & Maddocks, 2017). Additionally, serine protease is involved in tumor invasion and metastasis in oncogenesis (Sanguedolce et al., 2015). On the other hand, threonine is an essential amino acid that is crucial for the formation of various building blocks of proteins, including tooth enamel, collagen, and elastin. It also plays an essential role in the nervous system and several metabolic pathways. Both serine and threonine are critical elements of a serine/threonine-protein kinase, which has been identified as a potential biomarker for bladder cancer (Hentschel et al., 2021). The increased levels of both serine and threonine in our study were also observed by other researchers in blood serum (Amara et al., 2019; Vantaku et al., 2019) and also in urine (Kim et al., 2010).

Utilizing modified silver-109 targets in LDI-MS experiments enabled to measure the amount of polar and non-polar metabolites in tissue extracts. By employing this approach,

analysis of tissue metabolites using MS allowed for the identification of 31 compounds that exhibited lower abundance in cancer tissue in comparison to normal while one compound was found to be present in higher concentrations. Most of these compounds were putatively identified as peptides and lipids.

In our studies, we observed significantly lower levels of eight specific peptides in tumor tissue compared to adjacent normal tissue (Table S5). This observation could indicate a shift in protein metabolism within the cancer cells. In general, in many types of cancer, increased expression of certain peptides and proteins is often observed, which is associated with the activation of various signaling and metabolic pathways supporting the growth and survival of cancer cells (Lucarelli et al., 2018). However, our observation of decreased peptide levels could signify an enhanced protein catabolism. This process involves the breakdown of proteins to supply amino acids, which are then utilized for synthesizing new proteins and meeting other metabolic demands of the cancer cells. Therefore, the observed reduction in peptide levels in tumor tissues may be indicative of this heightened protein turnover, characterized by a rapid degradation of proteins and the repurposing of their constituents to support the proliferative and growth needs of the cancer cells.

The volume of research focusing on lipid metabolism and its association with urinary tract cancers has been steadily increasing. This burgeoning interest underscores the critical role of lipid metabolic pathways in the development and progression of these malignancies (Bombelli et al., 2020; di Meo et al., 2023). In our study, among the lipids found to be elevated in the normal tissue of BC patients, four belonged to the fatty acyl group while the remaining three were classified as diradylglycerols and one as a glycerophosphocholine. The level of lipids in cancerous tissues can be influenced by various factors, including altered metabolism, changes in lipid transport and uptake, and increased utilization of lipids for energy production (Cheng et al., 2018). As mentioned before cancer cells tend to exhibit increased aerobic glycolysis, also known as the Warburg effect, which can result in a reduction of lipid biosynthesis and accumulation in the cells (Broadfield et al., 2021). Additionally, cancer cells may rely on increased uptake of lipids from the extracellular environment to support their growth and proliferation. Moreover, cancer cells can utilize lipids as an energy source, which may contribute to a decrease in lipid levels in the tissue (Menendez & Lupu, 2007). The specific lipids identified and their reduced levels in tumor tissues suggest various metabolic alterations. For instance, the lower level of hydroxyisocaproic acid, a branched-chain fatty acid, might indicate a disruption in branched-chain fatty acid metabolism, a common occurrence in cancer (Ye et al., 2020). The eicosanoids, hydroxyeicosatetraenoic acid di-endoperoxide, and epoxy-7-eicosynoic acid, derived from arachidonic acid

and involved in inflammation and cell signaling, also showed reduced levels. This reduction could point to changes in eicosanoid metabolism, often associated with cancer progression and immune response (Johnson et al., 2020). The decreased level of specific diacylglycerols (DGs), crucial lipid signaling molecules, could suggest changes in signaling pathways linked to cell proliferation and survival (Cooke & Kazanietz, 2022). The last class of lipids identified in lower concentration in cancer tissues compared to normal tissues was glycerophosphocholine (GP). GPs are associated with phospholipid metabolism, and changes in this molecule could reflect alterations in membrane composition and signaling in cancer cells (Sonkar et al., 2019).

In an effort to identify cellular markers that could distinguish between the various grades and stages of BC, several metabolomics studies of the urine and blood of BC patients have been reported (Di Meo et al., 2022a, 2022b; Petrella et al., 2021). To our knowledge, however, only three studies have investigated the connections between changes in metabolite levels in tissues from BC patients and the distinct grades and/or stages of tumor development (Piyarathna et al., 2018; Sahu et al., 2017; Tripathi et al., 2013).

In our study, significantly higher concentrations of lactate and ethanolamine were measured in the HG cancer tissue of BC patients compared to the levels found in the normal tissue group (Fig. 3, Table 1). We found that lactate is one of the most differentiating metabolites between normal and neoplastic tissue, regardless of the stage of cancer. Ethanolamine is a component of certain phospholipids that make up the structure of cell membranes and plays an important role in the structure and function of cell membranes. These lipids are also involved in cell signaling and other cellular processes (Vance & Tasseva, 2013). In some types of cancer, there is evidence that the levels of ethanolamine differ significantly between samples collected from cancer patients compared to controls (Swanson et al., 2008). The higher level of ethanolamine may be related to the increased cell proliferation and growth that is characteristic of cancer. Cancer cells may require more ethanolamine to support the synthesis of new cell membranes and other cellular structures as they divide and multiply (Cheng et al., 2016).

Our research has identified a panel of 11 metabolites that, when considered together, may be good discriminators of low-grade cancer tissue versus adjacent normal tissue in bladder cancer patients. These metabolites include lactate, alanine, choline, glutamine, hypoxanthine, leucine, methionine, phenylalanine, serine, threonine, and tyrosine, eight of which are alpha-amino acids.

One of the most differentiating compounds between LG cancer and normal tissue from BC patients is choline. It is a crucial water-soluble quaternary amine that is often classified as a B vitamin due to its similar chemical structure. Choline has several important functions within the human

body, particularly in neurochemical processes (Tayebati et al., 2017). Choline plays a critical role in the production of phospholipids and the metabolism of triglycerides, making it essential for the proper structure and function of cell membranes. Our study found that cancer tissue from patients with bladder cancer had higher levels of choline compared to normal tissue, which could be due to increased absorption of choline by cancer cells. Our findings are consistent with previous research demonstrating that cancer cells tend to increase fatty acid synthesis, which can then act as a substrate for phosphatidylcholine synthesis, leading to its elevation in tumor cells (Koundouros & Poulougiannis, 2019; Saito et al., 2022). Interestingly, we observed the same trend in urine samples, with increased levels of choline observed in patients with BC (Li et al., 2021; Loras et al., 2019b). Moreover, one of our previous studies revealed that the increase in tissue choline levels among cancer patients is consistent with the decrease in choline levels found in the serum of patients with BC compared to control individuals (Ossoliński et al., 2022).

Our current study has indicated that tissue-based metabolite profiling can accurately discriminate different stages of cancer tissue (pTa and pT1) from normal tissue from BC patients (Table 1, Fig. 4). In the tissue extracts of patients with pTa and pT1 stages of BC, we identified 13 significant metabolites that were good discriminators of the different cancer stage groups compared to the normal tissue group, most of which are alpha-amino acids and have also been reported in the literature, as described above, in relation to the occurrence of cancer.

## 5 Conclusion

Our study has demonstrated that the combination of multivariate statistics, high-resolution NMR, and silver-109-based high-resolution LDI-MS metabolomics can effectively identify changes in tissue metabolome of patients with bladder cancer (BC). Using  $^1\text{H}$  NMR metabolomics, we identified six potentially robust metabolic indicators of BC, including lactate, glutamine, glutamate, hypoxanthine, serine, and threonine, which predicted BC with very good predictive power (AUC values  $> 0.853$ ). Furthermore, using silver-109 nanoparticle-based LDI-MS, we identified 34 additional compounds, mostly lipids, that helped differentiate between cancer and normal tissues. Additionally, we found thirteen metabolites that could potentially discriminate between low-grade and high-grade bladder cancer and thirteen metabolites that could serve as potential reporters of different grades of BC. Overall, our findings suggest that a combination of tissue metabolites has better predictive potential for diagnosing BC and evaluating disease severity and progression than using individual metabolites alone.

**Supplementary Information** The online version contains supplementary material available at <https://doi.org/10.1007/s11306-023-02076-w>.

**Acknowledgements** Research was supported mainly by National Science Centre (Poland), research project SONATA Number UMO-2018/31/D/ST4/00109. <sup>1</sup>H NMR spectra were recorded at Montana State University-Bozeman on a cryoprobe-equipped 600 MHz (14 Tesla) AVANCE III solution NMR spectrometer housed in MSU's NMR Center. Funding for MSU NMR Center's NMR instruments has been provided in part by the NIH SIG program (1S10RR13878 and 1S10RR026659), the National Science Foundation (NSF-MRI:DBI-1532078, NSF-MRI CHE: 2018388), the Murdock Charitable Trust Foundation (2015066:MNL), and support from the office of the Vice President for Research, Economic Development, and Graduate Education at MSU.

**Author contributions** Investigation: KO, TR, AP, AK, JN; Methodology: KO, TR, JN; Resources: KO, TR, VC, BPT, AO, TO, JN; Data Curation: TR, VC, BPT, JN, AK, AP; Formal analysis: JN; Visualization: JN, BPT; Writing—original draft: KO, ZK, JN; Writing—review and editing: VC, TR, BPT, JN; Supervision: JN, TR; Funding acquisition: JN, BPT, VC; Project administration: JN.

**Data availability** The data that support the findings of this study are available from the corresponding author upon reasonable request.

## Declarations

**Conflict of interest** The authors declare no competing financial and/or non-financial interests.

**Consent to participate** The patients provided written consent for participation in research.

**Consent for publication** The patients provided written informed consent for the publication of any associated data.

**Ethical approval** The study protocol was approved by local Bioethics Committee at the University of Rzeszow (Poland) (permission no. 2018/04/10).

**Research involving human and/or animal participants** This article does not contain any studies with human and/or animal participants performed by either of the authors.

## References

- Afonso, J., Santos, L. L., Longatto-Filho, A., & Baltazar, F. (2020). Competitive glucose metabolism as a target to boost bladder cancer immunotherapy. *Nature Reviews Urology*, *17*(2), 77–106. <https://doi.org/10.1038/s41585-019-0263-6>
- Alberice, J. V., Amaral, A. F. S., Armitage, E. G., Lorente, J. A., Algaba, F., Carrilho, E., et al. (2013). Searching for urine biomarkers of bladder cancer recurrence using a liquid chromatography–mass spectrometry and capillary electrophoresis–mass spectrometry metabolomics approach. *Journal of Chromatography A*, *1318*, 163–170. <https://doi.org/10.1016/J.CHROMA.2013.10.002>
- Amara, C. S., Ambati, C. R., Vantaku, V., Piyarathna, D. W. B., Donepudi, S. R., Ravi, S. S., et al. (2019). Serum metabolic profiling identified a distinct metabolic signature in bladder cancer smokers: A key metabolic enzyme associated with patient survival. *Cancer Epidemiology Biomarkers and Prevention*, *28*(4), 770–781. <https://doi.org/10.1158/1055-9965.EPI-18-0936/70061/AM/SERUM-METABOLIC-PROFILING-IDENTIFIED-A-DISTINCT>
- Bansal, N., Gupta, A., Mitash, N., Shakya, P. S., Mandhani, A., Mahdi, A. A., et al. (2013). Low- and high-grade bladder cancer determination via human serum-based metabolomics approach. *Journal of Proteome Research*, *12*(12), 5839–5850. [https://doi.org/10.1021/PR400859W/SUPPL\\_FILE/PR400859W\\_SI\\_001.PDF](https://doi.org/10.1021/PR400859W/SUPPL_FILE/PR400859W_SI_001.PDF)
- Benjamini, Y., Drai, D., Elmer, G., Kafkafi, N., & Golani, I. (2001). Controlling the false discovery rate in behavior genetics research. *Behavioural Brain Research*, *125*(1–2), 279–284. [https://doi.org/10.1016/S0166-4328\(01\)00297-2](https://doi.org/10.1016/S0166-4328(01)00297-2)
- Bianchi, C., Meregalli, C., Bombelli, S., Di Stefano, V., Salerno, F., Torsello, B., et al. (2017). The glucose and lipid metabolism reprogramming is grade-dependent in clear cell renal cell carcinoma primary cultures and is targetable to modulate cell viability and proliferation. *Oncotarget*, *8*(69), 113502. <https://doi.org/10.18632/ONCOTARGET.23056>
- Bombelli, S., Torsello, B., De Marco, S., Lucarelli, G., Cifola, I., Grasselli, C., et al. (2020). 36-kDa Annexin A3 isoform negatively modulates lipid storage in clear cell renal cell carcinoma cells. *The American Journal of Pathology*, *190*(11), 2317–2326. <https://doi.org/10.1016/J.AJPATH.2020.08.008>
- Broadfield, L. A., Pane, A. A., Talebi, A., Swinnen, J. V., & Fendt, S. M. (2021). Lipid metabolism in cancer: New perspectives and emerging mechanisms. *Developmental Cell*, *56*(10), 1363–1393. <https://doi.org/10.1016/J.DEVCEL.2021.04.013>
- Caspi, R., Billington, R., Fulcher, C. A., Keseler, I. M., Kothari, A., Krummenacker, M., et al. (2018). The MetaCyc database of metabolic pathways and enzymes. *Nucleic Acids Research*, *46*(D1), D633–D639. <https://doi.org/10.1093/nar/gkx935>
- Castelao, J. E., Yuan, J. M., Skipper, P. L., Tannenbaum, S. R., Gago-Dominguez, M., Crowder, J. S., et al. (2001). Gender- and smoking-related bladder cancer risk. *JNCI: Journal of the National Cancer Institute*, *93*(7), 538–545. <https://doi.org/10.1093/JNCI/93.7.538>
- Cheng, C., Geng, F., Cheng, X., & Guo, D. (2018). Lipid metabolism reprogramming and its potential targets in cancer. *Cancer Communications*, *38*(1), 1–14. <https://doi.org/10.1186/S40880-018-0301-4>
- Cheng, Y., Yang, X., Deng, X., Zhang, X., Li, P., Tao, J., et al. (2015). Metabolomics in bladder cancer: a systematic review. *International Journal of Clinical and Experimental Medicine*, *8*(7), 11052–11063.
- Cheng, M., Bhujwalla, Z. M., & Glunde, K. (2016). Targeting phospholipid metabolism in cancer. *Frontiers in Oncology*, *6*(Dec), 266. <https://doi.org/10.3389/FONC.2016.00266/BIBTEX>
- Cooke, M., & Kazanietz, M. G. (2022). Overarching roles of diacylglycerol signaling in cancer development and antitumor immunity. *Science Signaling*, *15*, 729. <https://doi.org/10.1126/SCISIGNAL.ABO0264/ASSET/FDC7EED-1DF7-4C5E-BD2F-E2E08F6DB403/ASSETS/IMAGES/LARGE/SCISIGNAL.ABO0264-F5.JPG>
- Danbolt, N. C. (2001). Glutamate uptake. *Progress in Neurobiology*, *65*(1), 1–105. [https://doi.org/10.1016/S0301-0082\(00\)00067-8](https://doi.org/10.1016/S0301-0082(00)00067-8)
- Dervisevic, M., Dervisevic, E., Azak, H., Çevik, E., Şenel, M., & Yildiz, H. B. (2016). Novel amperometric xanthine biosensor based on xanthine oxidase immobilized on electrochemically polymerized 10-[4H-dithieno(3,2-b:2',3'-d)pyrrole-4-yl]decane-1-amine film. *Sensors and Actuators b: Chemical*, *225*, 181–187. <https://doi.org/10.1016/J.SNB.2015.11.043>
- di Meo, N. A., Lasorsa, F., Rutigliano, M., Loizzo, D., Ferro, M., Stella, A., et al. (2022a). Renal cell carcinoma as a metabolic disease: An update on main pathways, potential biomarkers, and therapeutic targets. *International Journal of Molecular Sciences*, *23*(22), 14360. <https://doi.org/10.3390/IJMS232214360>

- di Meo, N. A., Lasorsa, F., Rutigliano, M., Milella, M., Ferro, M., Battaglia, M., et al. (2023). The dark side of lipid metabolism in prostate and renal carcinoma: Novel insights into molecular diagnostic and biomarker discovery. *Expert Review of Molecular Diagnostics*, 23(4), 297–313. <https://doi.org/10.1080/14737159.2023.2195553>
- Di Meo, N. A., Loizzo, D., Pandolfo, S. D., Autorino, R., Ferro, M., Porta, C., et al. (2022b). Metabolomic approaches for detection and identification of biomarkers and altered pathways in bladder cancer. *International Journal of Molecular Sciences*, 23(8), 4173. <https://doi.org/10.3390/IJMS23084173/S1>
- Emwas, A. H., Roy, R., McKay, R. T., Tenori, L., Saccenti, E., Nagana Gowda, G. A., et al. (2019). NMR spectroscopy for metabolomics research. *Metabolites*, 9(7), 123. <https://doi.org/10.3390/METABO9070123>
- Fischer, K., Hoffmann, P., Voelkl, S., Meidenbauer, N., Ammer, J., Edinger, M., et al. (2007). Inhibitory effect of tumor cell-derived lactic acid on human T cells. *Blood*, 109(9), 3812–3819. <https://doi.org/10.1182/BLOOD-2006-07-035972>
- Gao, H., Dong, B., Jia, J., Zhu, H., Diao, C., Yan, Z., et al. (2012). Application of ex vivo <sup>1</sup>H NMR metabolomics to the characterization and possible detection of renal cell carcinoma metastases. *Journal of Cancer Research and Clinical Oncology*, 138(5), 753–761. <https://doi.org/10.1007/s00432-011-1134-6>
- Garg, D., Singh, M., Verma, N., & Monika. (2022). Review on recent advances in fabrication of enzymatic and chemical sensors for hypoxanthine. *Food Chemistry*, 375, 131839. <https://doi.org/10.1016/J.FOODCHEM.2021.131839>
- Gatenby, R. A., Gawlinski, E. T., Gmitro, A. F., Kaylor, B., & Gillies, R. J. (2006). Acid-mediated tumor invasion: A multidisciplinary study. *Cancer Research*, 66(10), 5216–5223. <https://doi.org/10.1158/0008-5472.CAN-05-4193>
- Guin, S., Pollard, C., Ru, Y., Lew, C. R., Duex, J. E., Dancik, G., et al. (2014). Role in tumor growth of a glycogen debranching enzyme lost in glycogen storage disease. *JNCI Journal of the National Cancer Institute*. <https://doi.org/10.1093/JNCI/DJU062>
- Gupta, A., Bansal, N., Mitash, N., Kumar, D., Kumar, M., Sankhwar, S. N., et al. (2020). NMR-derived targeted serum metabolic biomarkers appraisal of bladder cancer: A pre- and post-operative evaluation. *Journal of Pharmaceutical and Biomedical Analysis*, 183, 113134. <https://doi.org/10.1016/J.JPBA.2020.113134>
- Hall, J. C., Heel, K., & McCauley, R. (1996). Glutamine. *The British Journal of Surgery*, 83(3), 305–312. <https://doi.org/10.1002/BJS.1800830306>
- Hentschel, A. E., van der Toom, E. E., Vis, A. N., Ket, J. C. F., Bosschieter, J., Heymans, M. W., et al. (2021). A systematic review on mutation markers for bladder cancer diagnosis in urine. *BJU International*, 127(1), 12–27. <https://doi.org/10.1111/BJU.15137>
- Ho, S. Y., Phua, K., Wong, L., & Bin Goh, W. W. (2020). Extensions of the external validation for checking learned model interpretability and generalizability. *Patterns*, 1(8), 100129. <https://doi.org/10.1016/J.PATTER.2020.100129>
- Hu, D., Xu, X., Zhao, Z., Li, C., Tian, Y., Liu, Q., et al. (2021). Detecting urine metabolites of bladder cancer by surface-enhanced Raman spectroscopy. *Spectrochimica Acta-Part a: Molecular and Biomolecular Spectroscopy*, 247, 119108. <https://doi.org/10.1016/j.saa.2020.119108>
- Jacyna, J., Kordalewska, M., Artymowicz, M., Markuszewski, M., Matuszewski, M., & Markuszewski, M. J. (2022). Pre- and post-resection urine metabolic profiles of bladder cancer patients: Results of preliminary studies on time series metabolomics analysis. *Cancers*, 14(5), 1210. <https://doi.org/10.3390/CANCE RS14051210>
- Jin, X., Yun, S. J., Jeong, P., Kim, I. Y., Kim, W. J., & Park, S. (2014). Diagnosis of bladder cancer and prediction of survival by urinary metabolomics. *Oncotarget*, 5(6), 1635. <https://doi.org/10.18632/ONCOTARGET.1744>
- Johnson, A. M., Kleczko, E. K., & Nemenoff, R. A. (2020). Eicosanoids in cancer: New roles in immunoregulation. *Frontiers in Pharmacology*, 11, 595498. <https://doi.org/10.3389/FPHAR.2020.595498/BIBTEX>
- Kim, J. W., Lee, G., Moon, S. M., Park, M. J., Hong, S. K., Ahn, Y. H., et al. (2010). Metabolomic screening and star pattern recognition by urinary amino acid profile analysis from bladder cancer patients. *Metabolomics*, 6(2), 202–206. <https://doi.org/10.1007/s11306-010-0199-6>
- Koundouros, N., & Pouligiannis, G. (2019). Reprogramming of fatty acid metabolism in cancer. *British Journal of Cancer*, 122(1), 4–22. <https://doi.org/10.1038/s41416-019-0650-z>
- Labow, B. I., & Souba, W. W. (2000). Glutamine. *World Journal of Surgery*, 24(12), 1503–1513. <https://doi.org/10.1007/S002680010269/METRCS>
- Lawal, A. T., & Adeloju, S. B. (2012). Progress and recent advances in fabrication and utilization of hypoxanthine biosensors for meat and fish quality assessment: A review. *Talanta*, 100, 217–228. <https://doi.org/10.1016/J.TALANTA.2012.07.085>
- Li, J., Cheng, B., Xie, H., Zhan, C., Li, S., & Bai, P. (2021). Bladder cancer biomarker screening based on non-targeted urine metabolomics. *International Urology and Nephrology*, 54(1), 23–29. <https://doi.org/10.1007/S11255-021-03080-6>
- Liu, X., Yao, D., Liu, C., Cao, Y., Yang, Q., Sun, Z., & Liu, D. (2016). Overexpression of ABCC3 promotes cell proliferation, drug resistance, and aerobic glycolysis and is associated with poor prognosis in urinary bladder cancer patients. *Tumor Biology*, 37(6), 8367–8374. <https://doi.org/10.1007/S13277-015-4703-5/FIGURES/4>
- Loras, A., Suárez-Cabrera, C., Martínez-Bisbal, M. C., Quintás, G., Paramio, J. M., Martínez-Máñez, R., et al. (2019a). Integrative metabolomic and transcriptomic analysis for the study of bladder cancer. *Cancers*. <https://doi.org/10.3390/cancers11050686>
- Loras, A., Suárez-Cabrera, C., Martínez-Bisbal, M. C., Quintás, G., Paramio, J. M., Martínez-Máñez, R., et al. (2019b). Integrative metabolomic and transcriptomic analysis for the study of bladder cancer. *Cancers*, 11(5), 686. <https://doi.org/10.3390/CANCE RS11050686>
- Loras, A., Trassiera, M., Sanjuan-Herráez, D., Martínez-Bisbal, M. C., Castell, J. V., Quintás, G., & Ruiz-Cerdá, J. L. (2018). Bladder cancer recurrence surveillance by urine metabolomics analysis. *Scientific Reports*, 8(1), 1–10. <https://doi.org/10.1038/s41598-018-27538-3>
- Lucarelli, G., Galleggiante, V., Rutigliano, M., Sanguedolce, F., Cagiano, S., Bufo, P., et al. (2015). Metabolomic profile of glycolysis and the pentose phosphate pathway identifies the central role of glucose-6-phosphate dehydrogenase in clear cell-renal cell carcinoma. *Oncotarget*, 6(15), 13371. <https://doi.org/10.18632/ONCOTARGET.3823>
- Lucarelli, G., Loizzo, D., Franzin, R., Battaglia, S., Ferro, M., Cantello, F., et al. (2019). Metabolomic insights into pathophysiological mechanisms and biomarker discovery in clear cell renal cell carcinoma. *Expert Review of Molecular Diagnostics*, 19(5), 397–407. <https://doi.org/10.1080/14737159.2019.1607729>
- Lucarelli, G., Rutigliano, M., Loizzo, D., di Meo, N. A., Lasorsa, F., Mastropasqua, M., et al. (2022). MUC1 tissue expression and its soluble form CA15-3 identify a clear cell renal cell carcinoma with distinct metabolic profile and poor clinical outcome. *International Journal of Molecular Sciences*, 23(22), 13968. <https://doi.org/10.3390/IJMS232213968/S1>
- Lucarelli, G., Rutigliano, M., Sallustio, F., Ribatti, D., Giglio, A., Signorile, M. L., et al. (2018). Integrated multi-omics characterization reveals a distinctive metabolic signature and the role of NDUFA4L2 in promoting angiogenesis, chemoresistance,

- and mitochondrial dysfunction in clear cell renal cell carcinoma. *Aging (Albany NY)*, 10(12), 3957. <https://doi.org/10.18632/AGING.101685>
- Massari, F., Ciccicarese, C., Santoni, M., Iacovelli, R., Mazzucchelli, R., Piva, F., et al. (2016). Metabolic phenotype of bladder cancer. *Cancer Treatment Reviews*, 45, 46–57. <https://doi.org/10.1016/j.ctrv.2016.03.005>
- Menendez, J. A., & Lupu, R. (2007). Fatty acid synthase and the lipogenic phenotype in cancer pathogenesis. *Nature Reviews Cancer*, 7(10), 763–777. <https://doi.org/10.1038/nrc2222>
- Montironi, R., & Lopez-Beltran, A. (2005). The 2004 WHO Classification of bladder tumors: A summary and commentary. *International Journal of Surgical Pathology*, 13(2), 143–153. <https://doi.org/10.1177/106689690501300203>
- Mushtaq, J., Thurairaja, R., & Nair, R. (2019). Bladder cancer. *Surface Science Reports*, 37(9), 529–537. <https://doi.org/10.1016/j.mpsur.2019.07.003>
- Newman, A. C., & Maddocks, O. D. K. (2017). Serine and functional metabolites in cancer. *Trends in Cell Biology*, 27(9), 645–657. <https://doi.org/10.1016/j.tcb.2017.05.001>
- Nizioł, J., Copié, V., Tripet, B. P., Nogueira, L. B., Nogueira, K. O. P. C., Ossoliński, K., et al. (2021). Metabolomic and elemental profiling of human tissue in kidney cancer. *Metabolomics*, 17(3), 30. <https://doi.org/10.1007/S11306-021-01779-2>
- Nizioł, J., Ossoliński, K., Plaza-Altamer, A., Kołodziej, A., Ossolińska, A., Ossoliński, T., & Ruman, T. (2022). Untargeted ultra-high-resolution mass spectrometry metabolomic profiling of blood serum in bladder cancer. *Scientific Reports*, 12(1), 1–13. <https://doi.org/10.1038/s41598-022-19576-9>
- Okuda, S., Yamada, T., Hamajima, M., Itoh, M., Katayama, T., Bork, P., et al. (2008). KEGG Atlas mapping for global analysis of metabolic pathways. *Nucleic Acids Research*, 36(suppl\_2), W423–W426. <https://doi.org/10.1093/NAR/GKN282>
- Omar, K., Khan, N. S., & Khan, M. S. (2019). Bladder neoplasm. *Blandy's Urology*. <https://doi.org/10.1002/9781118863343.CH21>
- Ossoliński, K., Ruman, T., Copié, V., Tripet, B. P., Nogueira, L. B., Nogueira, K. O. P. C., et al. (2022). Metabolomic and elemental profiling of blood serum in bladder cancer. *Journal of Pharmaceutical Analysis*, 12(6), 889–900. <https://doi.org/10.1016/j.jpha.2022.08.004>
- Pang, Z., Chong, J., Zhou, G., De Lima Morais, D. A., Chang, L., Barrette, M., et al. (2021). MetaboAnalyst 5.0: narrowing the gap between raw spectra and functional insights. *Nucleic Acids Research*, 49(W1), W388–W396. <https://doi.org/10.1093/NAR/GKAB382>
- Pasikanti, K. K., Esuvaranathan, K., Ho, P. C., Mahendran, R., Kamaraj, R., Wu, Q. H., et al. (2010). Noninvasive urinary metabolomic diagnosis of human bladder cancer. *Journal of Proteome Research*, 9(6), 2988–2995. <https://doi.org/10.1021/PR901173V>
- Petrella, G., Ciufolini, G., Vago, R., & Cicero, D. O. (2021). Urinary metabolic markers of bladder cancer: A reflection of the tumor or the response of the body? *Metabolites*, 11(11), 756. <https://doi.org/10.3390/METABO11110756>
- Piyarathna, D. W. B., Rajendiran, T. M., Putluri, V., Vantaku, V., Soni, T., von Rundstedt, F. C., et al. (2018). Distinct lipidomic landscapes associated with clinical stages of urothelial cancer of the bladder. *European Urology Focus*, 4(6), 907–915. <https://doi.org/10.1016/j.euf.2017.04.005>
- Plaza, A., Kołodziej, A., Nizioł, J., & Ruman, T. (2021). Laser ablation synthesis in solution and nebulization of silver-109 nanoparticles for mass spectrometry and mass spectrometry imaging. *ACS Measurement Science Au*, 2(1), 14–22. <https://doi.org/10.1021/ACSMEASURESCLAU.1C00020>
- Putluri, N., Shojaie, A., Vasu, V. T., Vareed, S. K., Nalluri, S., Putluri, V., et al. (2011). Metabolomic profiling reveals potential markers and bioprocesses altered in bladder cancer progression. *Cancer Research*, 71(24), 7376–7386. <https://doi.org/10.1158/0008-5472.CAN-11-1154>
- Ragone, R., Sallustio, F., Piccinonna, S., Rutigliano, M., Vanessa, G., Palazzo, S., et al. (2016). Renal cell carcinoma: A study through NMR-based metabolomics combined with transcriptomics. *Diseases*, 4(1), 7. <https://doi.org/10.3390/diseases4010007>
- Rodrigues, D., Jerónimo, C., Henrique, R., Belo, L., De Lourdes Bastos, M., De Pinho, P. G., & Carvalho, M. (2016). Biomarkers in bladder cancer: A metabolomic approach using in vitro and ex vivo model systems. *International Journal of Cancer*, 139(2), 256–268. <https://doi.org/10.1002/IJC.30016>
- Rosenstein, P. G., Tennent-Brown, B. S., & Hughes, D. (2018). Clinical use of plasma lactate concentration. Part 1: Physiology, pathophysiology, and measurement. *Journal of Veterinary Emergency and Critical Care*, 28(2), 85–105. <https://doi.org/10.1111/VECC.12708>
- Saginala, K., Barsouk, A., Aluru, J. S., Rawla, P., Padala, S. A., & Barsouk, A. (2020). Epidemiology of bladder cancer. *Medical Sciences*. <https://doi.org/10.3390/MEDSCI8010015>
- Sahu, D., Lotan, Y., Wittmann, B., Neri, B., & Hansel, D. E. (2017). Metabolomics analysis reveals distinct profiles of nonmuscle-invasive and muscle-invasive bladder cancer. *Cancer Medicine*, 6(9), 2106–2120. <https://doi.org/10.1002/CAM4.1109>
- Saito, R. F., Andrade, L. N. S., Bustos, S. O., & Chammas, R. (2022). Phosphatidylcholine-derived lipid mediators: The crosstalk between cancer cells and immune cells. *Frontiers in Immunology*. <https://doi.org/10.3389/FIMMU.2022.768606>
- Sanguedolce, F., Cormio, A., Bufo, P., Carrieri, G., & Cormio, L. (2015). Molecular markers in bladder cancer: Novel research frontiers. *Critical Reviews in Clinical Laboratory Sciences*, 52(5), 242–255. <https://doi.org/10.3109/10408363.2015.1033610>
- Siegel, R. L., Miller, K. D., Fuchs, H. E., & Jemal, A. (2022). Cancer statistics, 2022. *CA: A Cancer Journal for Clinicians*, 72(1), 7–33. <https://doi.org/10.3322/CAAC.21708>
- Sonkar, K., Ayyappan, V., Tressler, C. M., Adelaja, O., Cai, R., Cheng, M., & Glunde, K. (2019). Focus on the glycerophosphocholine pathway in choline phospholipid metabolism of cancer. *NMR in Biomedicine*, 32(10), e4112. <https://doi.org/10.1002/NBM.4112>
- Sud, M., Fahy, E., Cotter, D., Brown, A., Dennis, E. A., Glass, C. K., et al. (2007). LMSD: LIPID MAPS structure database. *Nucleic Acids Research*. <https://doi.org/10.1093/nar/gkl838>
- Sun, N., Liang, Y., Chen, Y., Wang, L., Li, D., Liang, Z., et al. (2019). Glutamine affects T24 bladder cancer cell proliferation by activating STAT3 through ROS and glutaminolysis. *International Journal of Molecular Medicine*, 44(6), 2189–2200. <https://doi.org/10.3892/IJMM.2019.4385/HTML>
- Sung, H., Ferlay, J., Siegel, R. L., Laversanne, M., Soerjomataram, I., Jemal, A., & Bray, F. (2021). Global Cancer Statistics 2020: GLOBOCAN Estimates of incidence and mortality worldwide for 36 cancers in 185 countries. *CA: A Cancer Journal for Clinicians*, 71(3), 209–249. <https://doi.org/10.3322/CAAC.21660>
- Swanson, M. G., Keshari, K. R., Tabatabai, Z. L., Simko, J. P., Shinohara, K., Carroll, P. R., et al. (2008). Quantification of choline- and ethanolamine-containing metabolites in human prostate tissues using 1H HR-MAS total correlation spectroscopy. *Magnetic Resonance in Medicine*, 60(1), 33–40. <https://doi.org/10.1002/MRM.21647>
- Tan, G., Wang, H., Yuan, J., Qin, W., Dong, X., Wu, H., & Meng, P. (2017). Three serum metabolite signatures for diagnosing low-grade and high-grade bladder cancer. *Scientific Reports*. <https://doi.org/10.1038/srep46176>
- Tayebati, S. K., Martinelli, I., Moruzzi, M., Amenta, F., & Tomasoni, D. (2017). Choline and choline alphoscerate do not modulate inflammatory processes in the rat brain. *Nutrients*, 9(10), 1084. <https://doi.org/10.3390/NU9101084>

- Tripathi, P., Somashekar, B. S., Ponnusamy, M., Gursky, A., Dailey, S., Kunju, P., et al. (2013). HR-MAS NMR tissue metabolomic signatures cross-validated by mass spectrometry distinguish bladder cancer from benign disease. *Journal of Proteome Research*, *12*(7), 3519–3528. [https://doi.org/10.1021/PR4004135/SUPPL\\_FILE/PR4004135\\_SI\\_001.PDF](https://doi.org/10.1021/PR4004135/SUPPL_FILE/PR4004135_SI_001.PDF)
- Vance, J. E., & Tasseva, G. (2013). Formation and function of phosphatidylserine and phosphatidylethanolamine in mammalian cells. *Biochimica Et Biophysica Acta (BBA)-Molecular and Cell Biology of Lipids*, *1831*(3), 543–554. <https://doi.org/10.1016/j.BBALIP.2012.08.016>
- Vantaku, V., Donepudi, S. R., Piyarathna, D. W. B., Amara, C. S., Ambati, C. R., Tang, W., et al. (2019). Large-scale profiling of serum metabolites in African American and European American patients with bladder cancer reveals metabolic pathways associated with patient survival. *Cancer*, *125*(6), 921–932. <https://doi.org/10.1002/CNCR.31890>
- Viswambaram, P., & Hayne, D. (2020). Gender discrepancies in bladder cancer: Potential explanations. *Expert Review of Anticancer Therapy*. <https://doi.org/10.1080/14737140.2020.1813029>
- Warburg, O. (1956). On respiratory impairment in cancer cells. *Science*, *124*(3215), 269–270. <https://doi.org/10.1126/SCIENCE.124.3215.269>
- Wishart, D. S., Tzur, D., Knox, C., Eisner, R., Guo, A. C., Young, N., et al. (2007). HMDB: The Human Metabolome Database. *Nucleic Acids Research*, *35*(Database), D521–D526. <https://doi.org/10.1093/nar/gkl923>
- Wittmann, B. M., Stirdivant, S. M., Mitchell, M. W., Wulff, J. E., McDunn, J. E., Li, Z., et al. (2014). Bladder cancer biomarker discovery using global metabolomic profiling of urine. *PLoS ONE*, *9*(12), e115870. <https://doi.org/10.1371/JOURNAL.PONE.0115870>
- Wong, M. C. S., Fung, F. D. H., Leung, C., Cheung, W. W. L., Goggins, W. B., & Ng, C. F. (2018). The global epidemiology of bladder cancer: A joinpoint regression analysis of its incidence and mortality trends and projection. *Scientific Reports*, *8*(1), 1–12. <https://doi.org/10.1038/s41598-018-19199-z>
- Ye, Z., Wang, S., Zhang, C., & Zhao, Y. (2020). Coordinated modulation of energy metabolism and inflammation by branched-chain amino acids and fatty acids. *Frontiers in Endocrinology*, *11*, 559087. <https://doi.org/10.3389/FENDO.2020.00617/BIBTEX>
- Zeki, Ö. C., Eylem, C. C., Reçber, T., Kır, S., & Nemutlu, E. (2020). Integration of GC–MS and LC–MS for untargeted metabolomics profiling. *Journal of Pharmaceutical and Biomedical Analysis*, *190*, 113509. <https://doi.org/10.1016/J.JPBA.2020.113509>
- Zhang, X. W., Li, Q. H., Xu, Z. D., & Dou, J. J. (2020). Mass spectrometry-based metabolomics in health and medical science: A systematic review. *RSC Advances*, *10*(6), 3092–3104. <https://doi.org/10.1039/C9RA08985C>

**Publisher's Note** Springer Nature remains neutral with regard to jurisdictional claims in published maps and institutional affiliations.

Springer Nature or its licensor (e.g. a society or other partner) holds exclusive rights to this article under a publishing agreement with the author(s) or other rightsholder(s); author self-archiving of the accepted manuscript version of this article is solely governed by the terms of such publishing agreement and applicable law.